Journal Pre-proof

IMPG2-related maculopathy

Johannes Birtel , Richard Caswell , Samantha R. De Silva , Philipp Herrmann , Salwah Rehman , Andrew J. Lotery , Omar A. Mahroo , Michel Michaelides , Andrew R. Webster , Robert E. MacLaren , Peter Charbel Issa

PII: S0002-9394(23)00422-1
DOI: https://doi.org/10.1016/j.ajo.2023.10.002
Reference: AJOPHT 12694

To appear in: *American Journal of Ophthalmology*

Received date: January 16, 2023
Revised date: October 1, 2023
Accepted date: October 1, 2023

Please cite this article as: Johannes Birtel , Richard Caswell , Samantha R. De Silva , Philipp Herrmann , Salwah Rehman , Andrew J. Lotery , Omar A. Mahroo , Michel Michaelides , Andrew R. Webster , Robert E. MacLaren , Peter Charbel Issa , IMPG2-related maculopathy, *American Journal of Ophthalmology* (2023), doi: https://doi.org/10.1016/j.ajo.2023.10.002

IMPG2-related maculopathy

Johannes Birtel[1,2,3,4], Richard Caswell[5], Samantha R. De Silva[1,2,6,7], Philipp Herrmann[4], Salwah Rehman[1,2], Andrew J Lotery[8,9], Omar A. Mahroo[6,7], Michel Michaelides[6,7], Andrew R. Webster[6,7], Robert E MacLaren[1,2], Peter Charbel Issa[1,2]

[1] *Oxford Eye Hospital, Oxford University Hospitals NHS Foundation Trust, Oxford, United Kingdom*
[2] *Nuffield Laboratory of Ophthalmology, Nuffield Department of Clinical Neurosciences, University of Oxford, Oxford, United Kingdom*
[3] *Department of Ophthalmology, University Medical Center Hamburg-Eppendorf, Hamburg, Germany*
[4] *Department of Ophthalmology, University of Bonn, Bonn, Germany*
[5] *Exeter Genomics Laboratory, Royal Devon University Healthcare NHS Foundation Trust, Exeter, United Kingdom.*
[6] *Moorfields Eye Hospital NHS Foundation Trust, London, United Kingdom*
[7] *UCL Institute of Ophthalmology, University College London, London, United Kingdom*
[8] *Clinical Neurosciences, Clinical and Experimental Sciences, Faculty of Medicine, University of Southampton, Southampton, United Kingdom*
[9] *Southampton Eye Unit, University Hospital Southampton NHS Foundation Trust, Southampton, United Kingdom*

Surnames are underlined.

Short title: *IMPG2*-related maculopathy

Supplemental Material available at AJO.com

Corresponding author:
Peter Charbel Issa
Oxford Eye Hospital
John Radcliffe Hospital
Oxford OX3 9DU
United Kingdom
Telephone: +44 1865 234 737
E-mail: peter.issa@gmx.de

Abstract

Purpose: To investigate the phenotype, variability and penetrance of *IMPG2*-related maculopathy.

Design: Retrospective observational case series.

Methods: Clinical evaluation, multimodal retinal imaging, genetic testing, and molecular modeling.

Results: Twenty-five individuals with a mono-allelic *IMPG2* variant were included, 5 of whom were relatives of patients with *IMPG2*-associated retinitis pigmentosa. In 17 individuals (median age, 52 years; range, 20-72 years), a distinct maculopathy was present and included foveal elevation with or without subretinal vitelliform material or focal atrophy of the retinal pigment epithelium. Best corrected visual acuity (BCVA) was ≥ 20/50 in the better eye (n=15) and 5 patients were asymptomatic. Longitudinal observation (n=8, up to 19 years) demonstrated stable maculopathy (n=3), partial/complete resorption (n=4) or increase (n=1) of the subretinal material, with overall stable vision (n=6). The remaining 8 individuals (median age, 58 years; range, 43-83 years; BCVA ≥ 20/25) showed no manifest maculopathy and were identified through segregation analysis. All 8 were asymptomatic, with minimal foveal changes observed on optical coherence tomography in 3 cases. Eighteen different variants were detected, 11 of them truncating. Molecular modeling of five missense variants, c.727G>C, c.1124C>A, c.2816T>A, c.3047T>C and c.3193G>A supported the hypothesis that these have a loss-of-function effect.

Conclusions: Mono-allelic *IMPG2* variants may result in haplo-insufficiency manifesting as a maculopathy with variable penetrance and expressivity. Family members of patients with *IMPG2*-related retinitis pigmentosa may present with vitelliform lesions. The maculopathy often remains limited to the fovea and is usually associated with moderate visual impairment.

INTRODUCTION

Vitelliform lesions in the macular area may have diverse causes, and an exact pathophysiological classification is sometimes challenging. In general, they can be classified as monogenic disorders associated with disease-causing variants in *BEST1*, *PRPH2*, *IMPG1* and *IMPG2*, or secondary, for instance associated with specific drusen subtypes or due to tractional photoreceptor – retinal pigment epithelium (RPE) separation.[1] Of the above genes, there is currently least information in the literature regarding *IMPG2*-related vitelliform lesions.[2-9]

IMPG2 encodes interphotoreceptor matrix proteoglycan-2 which is part of the retinal extracellular matrix that surrounds the photoreceptor inner and outer segments, as well as the apical processes of the RPE.[10-13] It has been demonstrated that mono-allelic *IMPG2* variants may be associated with vitelliform macular lesions,[1, 3-9] whereas bi-allelic variants result in retinitis pigmentosa (RP) with early-onset macular atrophy.[2, 5, 14-16] Truncating variants were found in both disease entities, indicating that haploinsufficiency may be the underlying mechanism in patients with *IMPG2*-related maculopathy. Hence, heterozygous carriers from families with *IMPG2*-related RP have a risk of developing retinal changes in adulthood.[4, 5]

Little is currently known about the penetrance or variability in expression of *IMPG2*-related maculopathy. Moreover, it has not been established if family members of patients with *IMPG2*-related RP who carry only one of the variants consistently develop vitelliform macular lesions.

In this study, we used multimodal imaging for a detailed phenotypic characterization of *IMPG2*-related maculopathy and investigated the presence and severity of macular disease in family members of patients with *IMPG2*-related retinopathy. Our findings have implications for patient and family counseling and illustrate how phenotyping may potentially inform us with regards to the pathogenicity of newly identified *IMPG2* variants.

METHODS

This retrospective study was conducted in adherence to the declaration of Helsinki. Clinical examination and genetic testing were performed as part of routine clinical care.[17] The study was approved by the institutional review board (Ethikkommission, University of Bonn #316/11; Ethikkommission Ärztekammer Hamburg, 2023-200751).

Assessment in each patient included best-corrected visual acuity (BCVA) testing, anterior segment and dilated fundus examination. Full-field electroretinography (ERG) and electro-oculography (EOG) was performed in selected cases. Retinal imaging included fundus photography, ultra-widefield pseudocolor and autofluorescence (AF) fundus imaging (Optos PLC, Dunfermline, United Kingdom), spectral-domain optical

coherence tomography (OCT), and fundus AF imaging with blue excitation light (both, Spectralis HRA+OCT, Heidelberg Engineering, Heidelberg, Germany).[18] Genetic testing was performed as described previously.[4, 19]

For protein modeling, in the absence of experimental structures for any part of the IMPG2 protein, analysis of missense variants was performed using the AlphaFold-2 model AF-Q9BZV3-F1.[20] After removal of extended regions of low confidence prediction (pLDDT score <70) from the model, analysis was performed on two regions, spanning residues 239-388, covering the first SEA (sea urchin sperm protein, enterokinase, agrin) domain and C-terminal flanking residues, and residues 897-1130, spanning the second SEA domain, EGF (epidermal growth factor)-like domains 1 and 2 and the transmembrane region. All positions of variants and their flanking residues were predicted in the AlphaFold model with pLDDT scores >70, the recommended minimum threshold for reliable analysis.[21] *In silico* mutagenesis was performed using the FoldX modeling suite,[22] and structures visualized in PyMOL (PyMOL Molecular Graphics System, Version 2.0, Schrödinger LLC; New York, NY, USA).

Results

Twenty-five individuals with a mono-allelic *IMPG2* variant were included in this study (Table 1). A distinct maculopathy was present in 17 patients (Figure 1, Supplementary Figures 1, 2) and included foveal elevation with or without subretinal vitelliform material or focal atrophy of the RPE. The remaining 8 individuals harboring an *IMPG2* variant demonstrated no or minimal foveal changes (Figure 2, Supplementary Figure 3); these individuals were identified in the context of segregation analysis which was performed in 9 families (pedigrees shown in Supplementary Figure 4). There was substantial overlap between the age range of those with and without macular disease (Supplementary Figure 5). Genetically tested family members without *IMPG2* variants (n=4, families 2, 3, 4, 15) showed no macular pathology (Supplementary Figure 4).

Five out of the 25 individuals were relatives of 3 patients with *IMPG2*-associated RP (Supplementary Figure 6) and carried only one of the index patient's *IMPG2* variants. Two of them presented with a vitelliform foveal lesion (#14-son, 14-dau), whereas the other 3 showed no foveal changes consistent with a vitelliform lesion (#15-mot, 15-bro, 16-mot).

Patients with maculopathy

Median age at first presentation was 52 years (range, 26-72 years). First symptoms occurred at a median age of 45 years (range, 25-71 years) and included distorted vision and reduced BCVA. Five patients with maculopathy were asymptomatic. BCVA in the better eye was 20/50 or better in all except 2 patients (#11, 12; Table 1), which is in line with previous publications (Supplementary Figure 7). Due to overall high symmetry of

the macular phenotype between right and left eyes, findings are reported for patients rather than for individual eyes.

In 11 patients, clinical examination demonstrated a yellowish vitelliform lesion in the central retina corresponding to foveal detachment of the neurosensory retina with subretinal hyperreflective material on OCT imaging. On fundus AF imaging, this hyperreflective material was associated with increased AF, except in 2 patients where macular pigment likely masked this effect (#2, 13). In 6 patients (#4, 5, 7, 10, 11, 12), a foveal detachment without relevant subretinal hyperreflective material on OCT was associated with central hypo- and hyperpigmentation on fundus photography and with areas of increased and decreased fundus AF. Overall, the foveal outer nuclear layer (ONL) and ellipsoid zone (EZ) appeared relatively well-preserved on OCT, but relative thinning of the ONL was prevalent in those with substantial or no subretinal hyperreflective material. OCT images also revealed mild irregularities of the foveal RPE layer in most eyes and there was a variable degree of increased choroidal reflectance (#1, 2, 4, 5, 9, 10, 11, 12, 13), indicating degenerative changes of the overlying RPE. One patient (#2) also showed small drusen-like lesions associated with pinpoint increased AF adjacent to the vitelliform deposits. These small lesions showed no obvious correlate on OCT. Another patient (#10) demonstrated reticular pseudodrusen. None of the patients showed signs of an active or fibrosed macular neovascular membrane. Only one eye (#3, left eye) showed an epiretinal membrane at baseline and there were no instances of vitreomacular traction that we judged could have caused a foveal detachment. Full-field ERG and EOG testing revealed normal responses in all tested individuals (n=9; Table 1).

Follow-up data were available for 8 patients (Figure 3) over a median observation period of 5 years (range, 2-16 years). Retinal changes appeared to be overall stable in 2 patients (observation period: 2 and 5 years). Subfoveal material at baseline partially or completely resorbed over time in 6 eyes of 5 patients (#1-5), increased in the right eye of 1 patient (#6), and became less well-defined in 1 eye (#3). The foveal RPE showed increased irregularities over time in 5 eyes of 3 patients (#1, 6, 11) and developed atrophy in 1 eye (#2). Although mild changes in BCVA of 1-2 lines were observed in several eyes, a loss of 3 lines or more occurred only in the eye with substantial increase of subfoveal material (#6) and in an eye which developed an anterior ischemic optic neuropathy. One patient (#3) developed a macula-off retinal detachment in her right eye which subsequently showed a marked reduction of the subretinal material. Six eyes of 5 patients (right eye of #5 and #7, left eye of #2 and 6, both eyes of #11) showed no obvious changes over the observational period.

Subjects with no or minimal foveal changes

Segregation analysis identified 8 asymptomatic family members (median age, 58 years; range, 43-83 years) with a mono-allelic *IMPG2* variant but no or minimal foveal changes (Table 1, Supplementary Figure 4). Visual acuity was 20/25 or better in all eyes, except for one eye of the 80-year-old patient (#15-mot) who presented with neovascular age-

related macular degeneration (AMD) which we interpreted as being unrelated to her *IMPG2* variant. Intermediate AMD was diagnosed in the 83-year-old patient (#16-mot). In all others, fundoscopy revealed no obvious macular abnormalities. OCT (Figure 3) demonstrated minimal foveal changes (n=3, #1-sis, 2-dau, 4-bro) at the interface between the EZ and interdigitation zone, including a mildly granular appearance, an abnormal foveal line with increased reflectivity between EZ and interdigitation zone, or a possible mild elevation of the EZ. AF images appeared normal overall, with only a few small spots of increased AF (n=4) without structural correlates on OCT – potentially within the limits of normal variation (Supplementary Figure 8). Longitudinal observation over 2 years in 3 individuals (Supplementary Figure 9) showed a reduction of a very mild elevation of the EZ in 1 eye (#1-sis) and the development of a faint line with increased reflectivity between the foveal EZ and interdigitation zone (#4-dau).

Structural context and impact of missense variants

The domain architecture of IMPG2, as annotated in the UniProtKB database (https://www.uniprot.org), is shown in Figure 4A, along with positions of variants described in this report. Missense variants p.Ala243Pro, p.Leu939His, p.Phe1016Ser and p.Gly1065Arg all lie within conserved functional domains as annotated in the UniProtKB database entry for IMPG2 (https://www.uniprot.org/uniprotkb/Q9BZV3/entry), namely the first and second SEA domains, and the first and second EGF-like domains, respectively (figure 4B, C). The p.Pro375Gln variant lies C-terminal of the first SEA domain as currently annotated. However, alignment of the predicted structures of the two SEA domains suggests that the first of these is an interrupted domain, containing an insertion of approximately 35 amino acids (residues 315-349) that is not present in the second, canonical-type domain (Supplementary Figure 10). Furthermore, residues 350-388 are predicted to form the second α-helix and 4th β-strand of the characteristic SEA domain structure, with Pro375 lying in the loop between these two features and thus likely forming part of the core SEA domain at the structural level. Interestingly, re-annotation of residues 239-388 as forming the core of SEA domain 1 would also place the previously-reported pathogenic missense variant p.(Ser379Pro) within this domain,[14] and in a position which would be likely to result in structural disruption (data not shown).

Within the first SEA domain, the p.Ala243Pro variant lies in the first strand of the β-sheet region. In the native structure, backbone atoms of Ala243 were predicted to form two inter-strand hydrogen bonds to the backbone of Val311, and these bonds are characteristic of the geometry of β-sheets (Supplementary Figure 11A). In the variant however, the cyclic nature of the proline sidechain means the variant residue is able to form only one inter-strand hydrogen bond (Supplementary Figure 11B), while constrained bond angles around the α-carbon atom are also unfavorable for the geometry of β-sheets, and for this reason proline is not generally found within β-strands.[23] As a result, the p.(Ala243Pro) substitution would be expected to destabilize the core structure of the SEA domain, resulting in a reduced level of functional protein.

As described above, in the predicted structure of the first, non-canonical SEA domain, Pro375 lies at the apex of a loop between the second α-helix and strand 4 of the β-sheet, where the non-polar cyclic sidechain of proline is directed into the hydrophobic interior of the domain and is closely surrounded by non-polar sidechains of other residues (Supplementary Figure 11C). The p.(Pro375Gln) substitution introduces a longer sidechain into this environment, which was predicted to be structurally destabilizing partly due to steric clashes between the novel glutamine sidechain and those of surrounding residues, but primarily due to the unfavorable introduction of the polar amide group into the hydrophobic protein core (Supplementary Figure 11D). The variant would thus likely reduce the efficiency of correct protein folding of the domain, resulting in a reduced level of functional protein. However, as the substitution occurs in a flexible loop, it is possible that the variant could, during folding, adopt an alternative structure with the novel glutamine sidechain facing outwards where it could interact favorably with water molecules. Such a conformation would likely be intrinsically less stable than that of the native structure, due to loss of van der Waals contacts between the proline sidechain and those of surrounding residues, but would negate the strong destabilizing effect arising from placement of the polar glutamine sidechain in the hydrophobic protein core.

Residues Leu939 and Phe1065 are strongly hydrophobic amino acids, both of which lie buried in the protein core; Leu939 lies in the long α-helix of SEA domain 2 (Supplementary Figure 11E), while Phe1065 lies in the first EGF-like domain, at an inter-domain interface with the second SEA domain (Supplementary Figure 11G). In both cases, variants at these positions introduce a polar amino acid into the protein core (histidine or serine, respectively), and were predicted to be destabilizing as a result (Supplementary Figure 11F, H). In the case of the p.Phe1016Ser variant, the predicted destabilization would be made more severe by the loss of non-bonded (or van der Waals) contacts with neighboring amino acid chains.

Gly1065 lies within the second EGF-like domain, in a loop just N-terminal of the first β-strand; this loop is stabilized by a disulphide bond between Cys1061 within the loop and Cys1077 in strand 2, while two other disulphide bonds also contribute to the stability of the core domain (Supplementary Figure 11I). Notably, the predicted positions of these disulphide bonds in the AlphaFold model were all consistent with prior annotation of the domain based on sequence homology, and with structural alignment of the model with known structures of other EGF-like domains. In the predicted structure of the native domain, the sharp turn of the loop is made possible by the lack of a sidechain in Gly1065. In the variant however, the bulky, charged sidechain of arginine would be forced into the confined interior of the loop where it was predicted to be severely destabilizing due to steric clashes with several surrounding groups, including residues of the Cys1079-Cys1092 disulphide bond (Supplementary Figure 11J). *In vivo*, the likelihood is that the substitution would prevent correct formation of the loop, thus preventing proper formation of disulphide bonds and so resulting in mis-folding and instability of the domain.

Discussion

In this study, we provide a detailed characterization of *IMPG2*-associated maculopathy, which is important to consider in the differential diagnosis of bilateral vitelliform maculopathy. All patients reported to date, and herein, demonstrated only mild visual symptoms. Long-term follow up data reported in this study with observation periods of up to 19 years, and the description of patients in their eighth decade, confirm that patients with *IMPG2*-associated maculopathy experience only moderate visual impairment and that retinal changes usually remain limited to the fovea. Relatively well-preserved BCVA is in line with previous reports, confirming the often good prognosis.[3-7, 9] Although secondary macular neovascularizations were not observed in this cohort and – to our knowledge – have not yet been reported in the literature, rare such instances cannot be excluded due to the currently only small number of reported cases.

When patients with *IMPG2*-associated maculopathy become visually symptomatic, a foveal detachment with or without subretinal vitelliform material is usually present. Examination of asymptomatic family members with a disease-causing *IMPG2*-variant allowed us to detect earlier, asymptomatic macular changes. In this cohort, the earliest likely *IMPG2*-associated foveal changes were detected on OCT and included fading or loss of the interdigitation zone, irregular hyperreflective changes between the EZ and interdigitation zone, an increased space between the EZ and RPE in the foveal center, and a faint hyperreflective band within this space. Notably, there were no associated abnormalities on AF imaging and fundoscopy. Whether or not these mild foveal changes are predictive of vitelliform lesion development remains to be explored in future longitudinal studies.

Foveal vitelliform lesions appear to develop via a common mechanism: a foveal elevation caused by separation of photoreceptors from the RPE is followed by accumulation of vitelliform material; presumably due to lack of phagocytosis of photoreceptor outer segments by the RPE. The vitelliform material is slowly cleared, leaving an elevated, thinned foveal photoreceptor layer and a slightly altered foveal RPE layer. The continued presence of the foveal EZ indicates some preserved structural integrity - a possible explanation for the relative preservation of BCVA. Diverging from this presumed disease course, the development of foveal RPE atrophy (#2) and spontaneous normalization of the foveal anatomy (#3), were observed in two subjects. The latter was preceded by a macula-off retinal detachment, but a direct effect of this event on the foveal lesion remains speculative.

An ancillary observation in one patient was the presence of small drusen-like lesions surrounding the foveal vitelliform lesion (#2). Similar pinpoint-sized changes with increased AF, but no obvious correlate on OCT, were also described in patients with *IMPG1*-related retinopathy, North Carolina macular dystrophy and benign yellow dot maculopathy.[3, 24, 25] Meunier et al. noted that similar lesions are usually not observed in patients with *BEST1*- and *PRPH2*-associated vitelliform dystrophies and hence might be useful for clinical differentiation. Whether or not scattered dots with increased AF observed in some family members without maculopathy are of any relevance in this context remains unclear.

The 80- and 83-year-old individuals we report harboring an *IMPG2* frame-shift (#15-mot) and truncating variant (#16-mot), respectively, were diagnosed with AMD, but showed no macular changes resembling *IMPG2*-associated disease, indicating incomplete penetrance. The other 3 individuals (#3-son, 4-dau, 15-bro) with an *IMPG2* variant but no foveal changes were younger (47, 42, and 43 years-of-age) and hence could still develop foveal lesions later in life. Three others (#1-sis, 2-dau, 4-bro) were of similar age as the index patient or older, but had very mild foveal changes only, indicating variable expressivity of *IMPG2*-associated maculopathy. Hence, as yet unknown genetic and/or environmental modifiers are likely, and predicting symptomatic disease due to *IMPG2* haploinsufficiency is currently not possible.

Variable effects of missense variants may add complexity. For instance, a homozygous missense variant (p.Phe124Leu), predicted to affect a highly conserved phenylalanine residue, was previously identified in a patient with a vitelliform macula phenotype.[2] If this variant was indeed disease-causing, this case would exemplify that the effect of bi-allelic mild variants may be comparable to a haploinsufficiency phenotype caused by monoallelic truncating mutations. Following such dose-effect logic, monoallelic truncating variants could be more penetrant than certain missense variants, if the latter result in only a partial loss-of-function. Nevertheless, our structural analysis of the five missense variants reported herein, p.(Ala243Pro), p.(Pro375Gln), p.(Leu939His), p.(Phe1016Ser) and p.(Gly1065Arg), indicated that all were likely to have a deleterious impact on protein structure and stability, leading to a reduced level of functional protein due to mis-folding and/or increased turnover. The predicted effect of these variants is therefore consistent with observed loss-of-function phenotypes and with previous reports of pathogenic missense variants within the affected domains.[4]

Patients with *IMPG2*-associated RP exhibit reduced night vision in the first two decades of life. Typically, these patients also have early macular involvement, ranging from mild pigmentary changes to profound chorioretinal atrophy with early loss of visual acuity.[2, 5, 14-16] A vitelliform phenotype in parents of an individual with RP (who would be of an appropriate age to exhibit vitelliform macular lesions) may clinically indicate the diagnosis of *IMPG2*-associated RP. Moreover, vitelliform lesions in family members may support pathogenicity of variants of unknown significance, or may indicate the likely presence of a second variant in RP patients with only one detected *IMPG2* variant.

As the loss of function mechanism in *IMPG2*-related retinopathy and the transgene size of about 3.7kb are suitable for retinal gene therapy using an AAV vector, this IRD might also be a candidate for gene therapy.[26] Proof of concept studies could be performed in RP patients, but the same strategy could be used for gene enhancement in patients with haploinsufficiency *IMPG2*-related maculopathy.

In summary, this study describes phenotypic characteristics in patients with *IMPG2*-related maculopathy and analysis of family members harboring a mono-allelic *IMPG2*-variant indicates variable penetrance and expressivity. Moreover, we present a unique familial constellation where vitelliform lesions may present in family members of patients with *IMPG2*-related RP. This supports previous work[5] that an ophthalmic examination in

family members of patients with *IMPG2* related rod-cone dystrophy may identify retinal changes, focus genetic counseling, and confirm the pathogenicity of *IMPG2* variants.

ACKNOWLEDGEMENTS / DISCLOSURES

Support: This work was supported by the Dr. Werner Jackstädt Foundation, Wuppertal, Germany (Grant S0134-10.22 to JB), and the National Institute for Health Research (NIHR) Oxford Biomedical Research Centre (BRC) and the NIHR BRC at Moorfields Eye Hospital and the UCL Institute of Ophthalmology. OAM is supported by the Wellcome Trust (206619/Z/17/Z). The views expressed are those of the authors and not necessarily those of the NHS, the NIHR or the Department of Health. The sponsor and funding organization had no role in the design or conduct of this research.

No financial disclosures exist for any author.

REFERENCES

1. Chowers I, Tiosano L, Audo I, Grunin M, Boon CJ. Adult-onset foveomacular vitelliform dystrophy: A fresh perspective. Prog Retin Eye Res 2015;47:64-85.
2. Bandah-Rozenfeld D, Collin RW, Banin E, et al. Mutations in IMPG2, encoding interphotoreceptor matrix proteoglycan 2, cause autosomal-recessive retinitis pigmentosa. Am J Hum Genet 2010;87:199-208.
3. Meunier I, Manes G, Bocquet B, et al. Frequency and clinical pattern of vitelliform macular dystrophy caused by mutations of interphotoreceptor matrix IMPG1 and IMPG2 genes. Ophthalmology 2014;121:2406-14.
4. Brandl C, Schulz HL, Charbel Issa P, et al. Mutations in the Genes for Interphotoreceptor Matrix Proteoglycans, IMPG1 and IMPG2, in Patients with Vitelliform Macular Lesions. Genes (Basel) 2017;8.
5. Khan AO, Al Teneiji AM. Homozygous and heterozygous retinal phenotypes in families harbouring IMPG2 mutations. Ophthalmic Genet 2019;40:247-251.
6. Shah SM, Schimmenti LA, Marmorstein AD, Bakri SJ. Adult-Onset Vitelliform Macular Dystrophy Secondary to a Novel Impg2 Gene Variant. Retin Cases Brief Rep 2021;15:356-358.
7. Vazquez-Dominguez I, Li CHZ, Fadaie Z, et al. Identification of a Complex Allele in IMPG2 as a Cause of Adult-Onset Vitelliform Macular Dystrophy. Invest Ophthalmol Vis Sci 2022;63:27.
8. Liu T, Aguilera N, Bower AJ, et al. Photoreceptor and Retinal Pigment Epithelium Relationships in Eyes With Vitelliform Macular Dystrophy Revealed by Multimodal Adaptive Optics Imaging. Invest Ophthalmol Vis Sci 2022;63:27.
9. Georgiou M, Chauhan MZ, Michaelides M, Uwaydat SH. IMPG2-associated unilateral adult onset vitelliform macular dystrophy. Am J Ophthalmol Case Rep 2022;28:101699.
10. Ishikawa M, Sawada Y, Yoshitomi T. Structure and function of the interphotoreceptor matrix surrounding retinal photoreceptor cells. Exp Eye Res 2015;133:3-18.
11. Acharya S, Foletta VC, Lee JW, et al. SPACRCAN, a novel human interphotoreceptor matrix hyaluronan-binding proteoglycan synthesized by photoreceptors and pinealocytes. J Biol Chem 2000;275:6945-55.
12. Kuehn MH, Stone EM, Hageman GS. Organization of the human IMPG2 gene and its evaluation as a candidate gene in age-related macular degeneration and other retinal degenerative disorders. Invest Ophthalmol Vis Sci 2001;42:3123-9.
13. Kuehn MH, Hageman GS. Molecular characterization and genomic mapping of human IPM 200, a second member of a novel family of proteoglycans. Mol Cell Biol Res Commun 1999;2:103-10.
14. van Huet RA, Collin RW, Siemiatkowska AM, et al. IMPG2-associated retinitis pigmentosa displays relatively early macular involvement. Invest Ophthalmol Vis Sci 2014;55:3939-53.
15. Bocquet B, Marzouka NA, Hebrard M, et al. Homozygosity mapping in autosomal recessive retinitis pigmentosa families detects novel mutations. Mol Vis 2013;19:2487-500.

16. Birtel J, Gliem M, Mangold E, et al. Next-generation sequencing identifies unexpected genotype-phenotype correlations in patients with retinitis pigmentosa. PLoS One 2018;13:e0207958.
17. Medical Research Council NHRA. Is my study research? 2017.
18. Birtel J, Yusuf IH, Priglinger C, Rudolph G, Charbel Issa P. Diagnosis of Inherited Retinal Diseases. Klin Monbl Augenheilkd 2021:249–260.
19. Birtel J, Eisenberger T, Gliem M, et al. Clinical and genetic characteristics of 251 consecutive patients with macular and cone/cone-rod dystrophy. Sci Rep 2018;8:4824.
20. Jumper J, Evans R, Pritzel A, et al. Highly accurate protein structure prediction with AlphaFold. Nature 2021;596:583-589.
21. Tunyasuvunakool K, Adler J, Wu Z, et al. Highly accurate protein structure prediction for the human proteome. Nature 2021;596:590-596.
22. Schymkowitz J, Borg J, Stricher F, Nys R, Rousseau F, Serrano L. The FoldX web server: an online force field. Nucleic Acids Res 2005;33:W382-8.
23. Li SC, Goto NK, Williams KA, Deber CM. Alpha-helical, but not beta-sheet, propensity of proline is determined by peptide environment. Proc Natl Acad Sci U S A 1996;93:6676-81.
24. Birtel J, Gliem M, Herrmann P, et al. North Carolina macular dystrophy shows a particular drusen phenotype and atrophy progression. Br J Ophthalmol 2021.
25. Dev Borman A, Rachitskaya A, Suzani M, et al. Benign Yellow Dot Maculopathy: A New Macular Phenotype. Ophthalmology 2017;124:1004-1013.
26. McClements ME, MacLaren RE. Adeno-associated Virus (AAV) Dual Vector Strategies for Gene Therapy Encoding Large Transgenes. Yale J Biol Med 2017;90:611-623.

Figure Legends

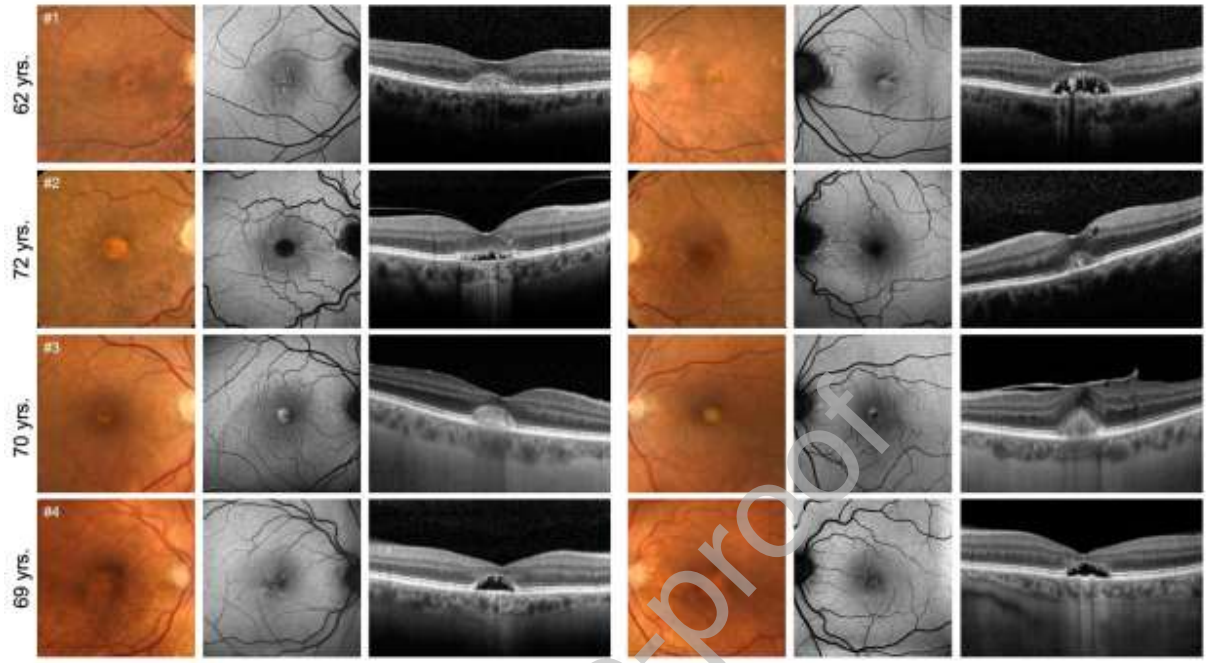

Figure 1: Retinal phenotype of patients with *IMPG2*-related maculopathy. Fundus color image (first and fourth column), fundus AF with 488 nm excitation light (second and sixth column), and horizontal spectral-domain OCT (third and seventh column) are shown.

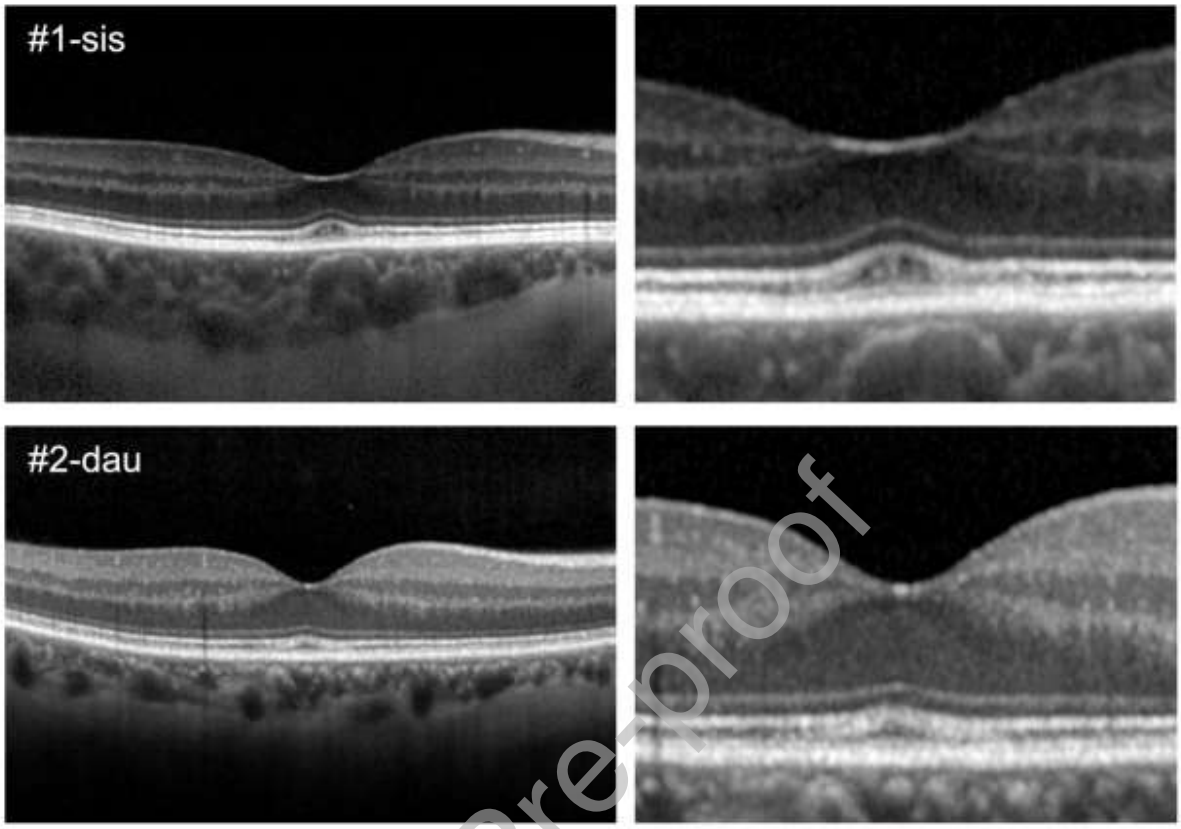

Figure 2: Horizontal spectral-domain OCT images of individuals with *IMPG2* variants and minimal foveal changes that are only visible on OCT images. These included a slightly elevated ellipsoid zone (#1-sis) and a thin reflective line between the ellipsoid and interdigitation zone (#2-dau).

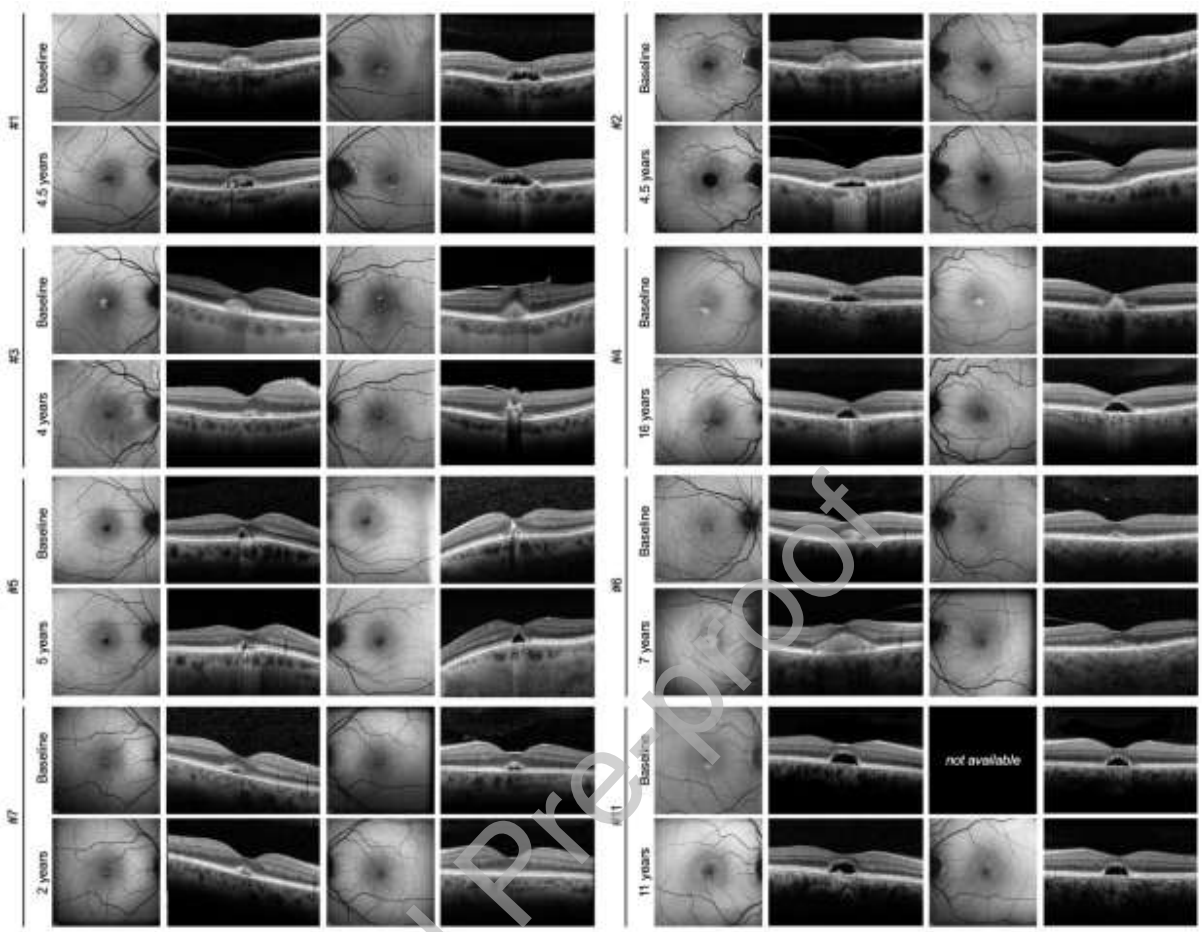

Figure 3: Longitudinal examination of patients with *IMPG2*-related maculopathy. Fundus AF with 488 nm excitation light (first and third column), and horizontal spectral-domain OCT (second and fourth column) are shown. The retinal thickening and vascular tortuosity in the right eye of #3 at follow up is caused by an eccentric epiretinal membrane that developed after retinal detachment surgery.

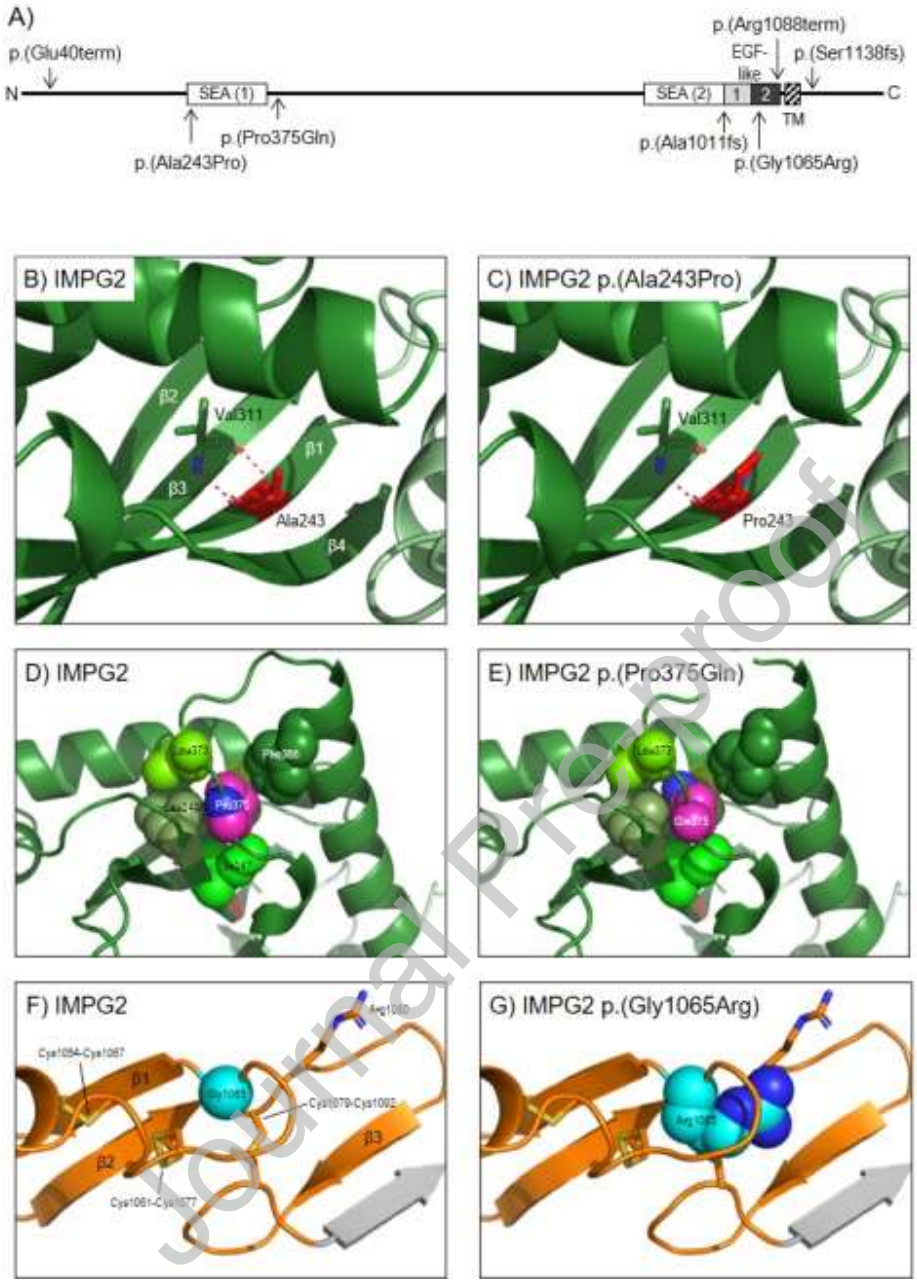

Figure 4: Location of identified missense variants in *IMPG2* and their predicted structural impact. A) Domain architecture of IMPG2 and location of variants. The thick black line represents the 1241-residue sequence of Interphotoreceptor matrix proteoglycan 2 (IMPG2), with solid boxes showing domains and regions as annotated in UniProtKB entry Q9BZV3: SEA (Sperm protein, Enterokinase and Agrin) domains 1 and 2 span residues 239-353 and 897-1010, respectively; EGF (epidermal growth factor)-like domains 1 and 2, residues 1010-1051 and 1052-1093; TM (transmembrane helix), residues 1100-1120; the dotted box extending C-terminal from SEA domain 1 shows revised annotation of the domain following structural alignment, which indicates the domain to span residues 239-386, including an insert relative to the canonical domain of

approximately 35 amino acids; positions of variants observed in cases reported here are shown either above (nonsense and frameshifting variants) or below (missense variants) the cartoon. B,C) AlphaFold-predicted structures of residues 239-388 (SEA domain 1), and residues 897-1130 (SEA domain 2, EGF-like domains 1 and 2, and TM helix; domains and regions are annotated by colour as labeled; sites of missense variants reported in this manuscript are colored cyan, with sidechains shown in stick format; sites of previously reported disease-associated missense variants are colored red; sidechains are also shown for disulphide-bonded cysteine residues in the EGF-like domains, a number of which are sites of pathogenic missense variants.

Identifier (#) / Family	Sex (m/f)	*IMPG2*-related maculopathy	Age at first symptoms	First examination		Last follow up examination		ffERG / EOG	Additional ocular conditions	*IMPG2*		
				Age	BCVA (R/L)	Age	BCVA (R/L)			Nucleotide	Protein	Reference
1	m	yes	60	62	20/25 20/40	66	20/40 20/50	n.a.	normal tension glaucoma	c.1124C>A	p.Pro375Gln	novel
1-sis	f	mfc	asymptomatic	64	20/25 20/25	66	20/25 20/20	n.a.	-			
2	f	yes	71	72	20/40 20/32	76	20/80[#] 20/32	n.a.	pseudophakia right AION (75 yrs)	c.3023-6_3030dup	p.Ala1011fs	novel
2-dau	f	mfc	asymptomatic	51	20/20 20/20	-	-	n.a.	-			
3	f	yes	69	70	20/32 20/40	74	20/25 20/50	n.a.	pseudophakia, right RD (73 yrs)	c.118G>T	p.Glu40*	1
3-son	m	no	asymptomatic	47	20/20 20/20	49	20/20 20/20	n.a.	-			
4	m	yes	41	50	20/50 20/40	69	20/40 20/63	n.a.	pseudophakia	c.3262C>T	p.Arg1088*	2, 3
4-dau	f	no	asymptomatic	42	20/20 20/20	44	20/25 20/20	n.a.	developed mfc			
4-bro	m	mfc	asymptomatic	64	20/20 20/20	-	-	n.a.	optic atrophy[+], pseudophakia			
5	f	yes	55	58	20/63 20/25	63	20/40 20/32	n.a.	-	c.3056del	p.Cys1019fs	novel
6	f	yes	asymptomatic	55	20/16 20/20	62	20/32 20/20	within normal limits	primary angle closure glaucoma	c.2588delG	p.Gly863Valfs*28	novel
7	f	yes	asymptomatic	38	20/20 20/20	40	20/20 20/20	within normal limits	-	c.3023-6_3030dup	p.Ala1011Phefs*2	novel
8	m	yes	55	60	20/32 20/40	-	-	n.a.	-	c.2268delT	p.Tyr756*	novel
8-son	m	yes	asymptomatic	32	20/32 20/20	-	-	within normal limits	-			

9	m	yes	asymptomatic	52	20/40 20/32	-	-	within normal limits	-	c.3634G>T	p.Glu1212*	4,5
10	f	yes	49	69	20/50 20/50	-	-	within normal limits	AMD	c.3047T>C	p.Phe1016Ser	6
11	f	yes	40	43	20/100 20/80	54	20/125 20/63	n.a.	right amblyopia	c.2143delT	p.Tyr715Thrfs*10	7,8
12	F	yes	30	50	20/63 20/63	-	-	within normal limits	-	c.2816T>A	p.Leu939His	novel
12-dau	F	yes	25	26	20/32 20/32	-	-	within normal limits	-			
13	M	yes	34	37	20/20 20/20	-	-	within normal limits	-	c.3262C>T	p.Arg1088*	2
14-son*	M	yes	40	54	20/50 20/32	-	-	within normal limits	-	c.727G>C	p.Ala243Pro	6
14-dau*	F	yes	asymptomatic	43	20/20 20/25	-	-	n.a.	-			
15-mot*	f	no	n.a.	80	20/40 20/20	-	-	n.a.	AMD right RAP	c.3413_3420delinsAATA	p.Ser1138fs	novel
15-bro*	m	no	asymptomatic	43	20/20 20/20	-	-	n.a.	-			
16-mot*	f	no	asymptomatic	83	20/25 20/20	-	-	n.a.	AMD, pseudophakia	c.1087C>T	p.Gln363*	novel

Table 1: Patient characteristics.

*ID-xxx describes the relation with the index patient (for pedigrees, see Supplementary Figure 4): dau = daughter, mot = mother, bro = brother, sis = sister, f = female; m = male; mfc = minimal foveal changes only on OCT imaging, likely representing very early IMPG2-related changes; R = right; L = left; ffERG = full field electroretinography; EOG = electro-oculography; n.a. = not available; HM = hand movements; LP = light perception; AMD = age-related macular degeneration; RAP = retinal angiomatous proliferation; RD = retinal detachment; AION = anterior ischemic optic neuropathy; OD = right eye, * = family member of patient with IMPG2-related retinitis pigmentosa; [+] = bilateral optic atrophy following a motorbike accident; [#] = visual deterioration following AION.*

1. Carss KJ, Arno G, Erwood M, et al. Comprehensive Rare Variant Analysis via Whole-Genome Sequencing to Determine the Molecular Pathology of Inherited Retinal Disease. Am J Hum Genet 2017;100:75-90.
2. Bandah-Rozenfeld D, Collin RW, Banin E, et al. Mutations in IMPG2, encoding interphotoreceptor matrix proteoglycan 2, cause autosomal-recessive retinitis pigmentosa. Am J Hum Genet 2010;87:199-208.
3. Khan AO, Al Teneiji AM. Homozygous and heterozygous retinal phenotypes in families harbouring IMPG2 mutations. Ophthalmic Genet 2019;40:247-251.
4. Ellingford; JM, Barton S, Bhaskar S, et al. Molecular findings from 537 individuals with inherited retinal disease. J Med Genet. 2016;53:761-767.
5. Stone EM, Andorf JL, Whitmore SS, et al. Clinically Focused Molecular Investigation of 1000 Consecutive Families with Inherited Retinal Disease. Ophthalmology. 2017;124:1314-1331
6. Brandl C, Schulz HL, Charbel Issa P, et al. Mutations in the Genes for Interphotoreceptor Matrix Proteoglycans, IMPG1 and IMPG2, in Patients with Vitelliform Macular Lesions. Genes (Basel) 2017;8.
7. Birtel J, Gliem M, Mangold E, et al. Next-generation sequencing identifies unexpected genotype-phenotype correlations in patients with retinitis pigmentosa. PLoS One. 2018;13:e0207958.
8. Colombo L, Maltese PE, Castori M, et al. Molecular Epidemiology in 591 Italian Probands With Nonsyndromic Retinitis Pigmentosa and Usher Syndrome. Invest Ophthalmol Vis Sci. 2021;62:13.

Table of contents statement

This study describes phenotypic characteristics of vitelliform maculopathy associated with monoallelic *IMPG2*-variants, including variable penetrance and expressivity. Family members of patients with *IMPG2*-related autosomal recessive retinitis pigmentosa may show such maculopathy, which may focus genetic testing, genetic counseling, and confirm the pathogenicity of *IMPG2* variants.